

Segmenting Cardiac MRI Tagging Lines using Gabor Filter Banks

Zhen Qian¹, Albert Montillo², Dimitris N. Metaxas¹ and Leon Axel³

¹Department of Biomedical Engineering, Rutgers University, Piscataway, NJ 08854, USA

²Department of Computer and Information Science, Univ. of Pennsylvania, Philadelphia, PA 19104, USA

³Department of Radiology, New York University, NY, NY 10016, USA

Abstract—This paper describes a new method for the automated segmentation and extraction of cardiac MRI tagging lines. Our method is based on the novel use of a 2D Gabor filter bank. By convolving the tagged input image with our Gabor filters, the tagging lines are automatically enhanced and segmented out. We design the Gabor filter bank based on the input image's spatial and frequency characteristics. The final result is a combination of each filter's response in the Gabor filter bank. We demonstrate that compared to bandpass filter methods such as HARP, this method results in robust and accurate segmentation of the tagging lines.

Keywords—Gabor filter bank, tagging line segmentation, tagged MRI images

I. INTRODUCTION

Tagged MRI is a non-invasive technique for the study of cardiac deformation. It generates an MRI-visible tag pattern within the cardiac tissue that deforms with the tissue during the cardiac cycle *in vivo* and gives motion information of the myocardium normal to the stripes (as shown in figure 1). A difficulty using this technique clinically is the lack of an efficient and robust post-processing method that can automatically segment and track over time the tagging lines.

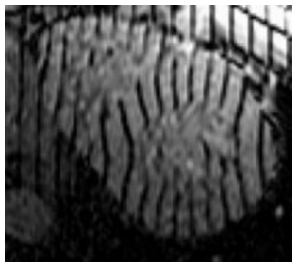


Figure 1: A tagged cardiac MRI

HARP [1] is an example of a technique that has been developed for rapid segmentation and analysis of tagged MR images. It generates phase angle images that roughly resemble the original tag pattern. Tagged MR images have a quasi-regular tagging pattern, which leads to relatively isolated peaks in their spectral domain. HARP is basically a bandpass filter that selectively filters those isolated spectral peaks. Although it provides a good direction towards the automated tagline segmentation, HARP has its limitations. Even with the addition of a Gaussian rolloff outside [2],

HARP's bandpass filter is still a relatively global transform in the spatial domain (as shown in figure 2), i.e., HARP's spatial local transform is affected by regions far away. Also, it is not obvious how to automatically design a bandpass filter that can simultaneously achieve good resolution in both the spatial and the frequency domains. When the first harmonic peak is not well concentrated, HARP has to increase the bandwidth of its bandpass filter. In this case, if the tagging lines deform a lot locally, it would not be robust to use such a wide bandpass filter, which cannot treat regions with and without tag deformations differently. Due to the phase-wrapping artifact [1], HARP is not suitable when large local deformations occur. Another limitation of HARP is that the synthetic tag lines obtained from the phase angle are an approximation to a tag line. Therefore it cannot represent its exact tagline shape, thickness and deformation.

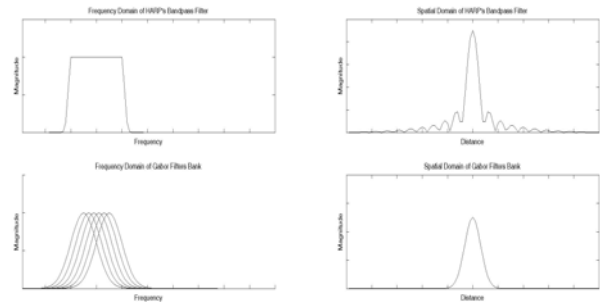


Figure 2: Simplified 1D model of HARP and Gabor filters in frequency domain (left) and spatial domain (right). Upper is HARP; lower is Gabor filter bank. A Gabor filter bank uses the combination of a group of Gabor filters to selectively cover the whole bandpass frequency range; each single filter can still get full constraints in its spatial domain.

In this paper, we describe a new method for the segmentation and extraction of tagging lines based on 2D Gabor filters. Gabor filters have been widely used in image processing applications, such as texture segmentation [3, 4, 5] and edge detection [6]. A main advantage of Gabor filters due to their Gaussian envelopes is that they always achieve the minimum space-bandwidth product which is specified in the uncertainty principle [4]. This advantage helps Gabor filters to get full constraints in their spatial domains (as shown in figure 2) as well as in their frequency domain. However, a bandpass method like HARP cannot achieve this. Gabor filters are wavelet-like local filters in the spatial domain, which makes it possible to design adaptive filters with respect to different spatial patterns of different local regions. In this paper we design a bank of Gabor filters with

different frequencies, directions and shapes which are specified according to the tag line pattern in the input image. We then convolve each Gabor filter in the filter bank with the input image, and derive our results by seeking the optimum filter for those pixels whose output is greater than a certain threshold. Therefore our result is a combination of those outputs from several Gabor filters (as shown in the lower-left part in figure 2). Our Gabor filter-based algorithm is adaptive because we specify the frequencies of interest locally rather than using a mixture of arbitrary frequencies as in HARP.

In the following sections, we first outline our theory and then we present some very promising experimental results of tagging line segmentation.

II. METHODOLOGY

2.1 Basic Definitions

The 2D Gabor filter was first introduced by Daugman [7]. It is basically a 2D Gaussian multiplied by a complex 2D sinusoid [3], as shown below:

$$h(x, y) = g(x', y') \cdot s(x, y) \quad (1)$$

where $g(x', y')$ is a 2D Gaussian, and $s(x, y)$ is a complex 2D sinusoid function, i.e.,

$$g(x', y') = \frac{1}{2\pi\sigma_x\sigma_y} \exp\left\{-\frac{1}{2}\left[\left(\frac{x'}{\sigma_x}\right)^2 + \left(\frac{y'}{\sigma_y}\right)^2\right]\right\}, \quad (2)$$

$$s(x, y) = \exp[-j2\pi(Ux + Vy)] \quad (3)$$

In (2):

$$x' = x \cos \theta + y \sin \theta, \quad y' = -x \sin \theta + y \cos \theta$$

are spatial coordinates which are rotated by an angle θ , and (σ_x, σ_y) gives the approximate spatial extent of the 2D Gaussian. Note that σ_x and σ_y need not be the same; thus the 2D Gaussian may not be symmetric. In (3), (U, V) are the 2D frequencies of the complex sinusoid, and its orientation is given by:

$$\phi = \arctan(V/U) \quad (4)$$

The Fourier transform $H(u, v)$ of $h(x, y)$ is given by:

$$H(u, v) = \exp\{-2\pi^2[(\sigma_x[u-U])^2 + (\sigma_y[v-V])^2]\} \quad (5)$$

Obviously, $H(u, v)$ is also a Gaussian whose center frequencies are (U, V) , and its frequency extent are determined by σ_x and σ_y . Thus, $H(u, v)$ is actually a bandpass filter. If we simplify our model to a symmetric Gaussian envelope, then $\sigma_x = \sigma_y = \sigma_h$, and from (5), we can get $H(u, v)$'s Gaussian standard deviation σ_H as $\sigma_H = 1/(2\pi \cdot \sigma_h)$. Thus:

$$\sigma_h \cdot \sigma_H = 1/2\pi \quad (6)$$

Thus the product of spatial resolution and frequency bandwidth achieves a minimum constant. This is why Gabor filters can simultaneously achieve optimal resolutions in both the spatial and the spatial-frequency domains.

2.2 Gabor Filters Bank Design for Tagging Line Segmentation

We use an ellipsoid-like 2D Gaussian envelope in our case (as shown in figure 3), which is more adaptive to the complicated geometries of cardiac tissues. We define the σ 's of the 2D Gaussian as in (7) and (8).

$$\sigma_x = \frac{1}{(U^2 + V^2)^{0.5}} \quad (7)$$

$$\sigma_y = \frac{1}{(U^2 + V^2)^{0.5}} \cdot \frac{1}{4} \quad (8)$$

where (U, V) are the frequencies of the fundamental harmonic of the input image. We obtain the (U, V) automatically by finding the coordinates of the fundamental harmonic peaks in the spectral domain [2].

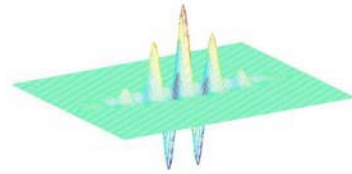


Figure 3: Real part of a Gabor filter in the spatial domain

The orientation angle θ of the Gaussian envelope is set equal to ϕ as was specified in (4). Thus with all the parameters specified above, we could set up a Gabor filter based on (1). Then we modulate parameters θ , U and V to generate a group of different Gabor filters based on the

features of the input image. The modified new θ' is set by $\theta' = \theta + \Delta\theta$, where $\Delta\theta$ varies from -30° to 30° . Thus different θ' could match different regions in the cardiac MRI (as shown in figure 4).



Figure 4: Different θ fits different cardiac region

Because the input images are taken during the systolic process, the spacing of tagging lines would change, and no longer be parallel. (as shown in figure 1). These changes in the spatial domain lead to corresponding changes in the frequency domain. The new U' and V' were specified as follows:

$$U' = \text{Re}\{(U + i \cdot V) \cdot m \cdot \exp(i \cdot \Delta\phi)\} \quad (9)$$

$$V' = \text{Im}\{(U + i \cdot V) \cdot m \cdot \exp(i \cdot \Delta\phi)\} \quad (10)$$

where m and $\Delta\phi$ are the magnitude and angle modulations respectively. We modulate m corresponding to the changes of tag spacing, and modulate $\Delta\phi$ corresponding to the changes of the tag lines' direction. For example, in figure 1, we set m to the range of $[0.9, 1.2]$, because during systole, most tag lines get closer to each other. And we set $\Delta\phi$ to vary from -10° to 10° by our observation of the tag lines directions change. Those Gabor filters whose $\theta' \cdot \Delta\phi < 0$ are excluded, because they can generate unacceptable artifacts.

As shown in (1), the Gabor filter is a Gaussian modulated by a sinusoid. We find a sinusoidal modulation of the Gaussian would only be desirable for finding a sinusoidal tag pattern. But real tagging lines are not exactly sinusoidal. As shown in figure 1, the tagging lines are usually thinner than the spacing in between. This is also why there exist second, third, or more, harmonics in the frequency domain. We try to modify the shape of the sinusoid by adding some higher harmonic components to it. Thus $s(x, y)$ is modified to:

$$s'(x, y) = \frac{1}{p} \exp\left\{-\frac{j\pi(Ux+Vy)(1+p)}{p}\right\}, \text{ when } \frac{1}{4\pi(1+p)} < |Ux+Vy| \leq \frac{2p+1}{4\pi(1+p)} ;$$

$$\exp\{-j\pi(1+p)(Ux+Vy)\}, \text{ when } \frac{1}{4\pi(1+p)} \geq |Ux+Vy|.$$

(11)

and $s'(x, y)$ is periodic with respect to $Ux + Vy$, whose period is $1/2\pi$.

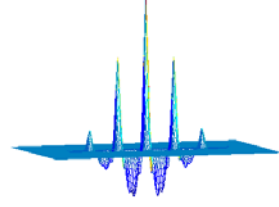


Figure 5: A modified Gabor with $p=3$.

We use p to control the sinusoid modification. p is the ratio of the sinusoid's negative domain to the positive domain. We set p based on the tagging patterns: p experimentally equals two times the ratio of the tag spacing to the tag thickness. Thus with respect to figure 1, we approximately set p to vary from 3 to 4.

2.3 Intensity Correction

Intensity inhomogeneity [8] is a common problem in MR images, which means different locations in the image have different intensity range (as shown in figure 1, the right top corner has much higher average intensity and contrast than the rest of the image).

We use a simple strategy to solve this problem. We assumed that the magnitude convolution result at a single pixel is a linear function of the local contrast near this pixel. To avoid artifacts from the contrast inhomogeneity, we simply adjust the resulting image by:

$$I' = I / I_c \quad (12)$$

where I_c is the smoothed image of the local contrast (as shown in figure 6).



Figure 6: Contrast Image I_c of figure 1

2.4 Normalization

The optimal thresholds for different Gabor filters vary. To determine the threshold of a certain Gabor filter, we must first do a normalization.

We assume that using different Gabor filters, the total number of pixels within the tag lines is a constant. First, the

total number (T) of the pixels in the tag lines is estimated in an initialization step. Then using different Gabor filters, we pick out for each filter the, $\alpha \cdot T$, number of pixels with highest value. Experimentally we set $\alpha=90\%$. The final result is a combination of all the results from each Gabor filter.

III. RESULTS

Figure 7a shows three short-axis cardiac MRI images during systole. Figure 7b shows the segmentation results using our method, where we set $-30^\circ \leq \Delta\theta \leq 30^\circ$, $\alpha=90\%$, $p=3$, and in (a1), $0.9 \leq m \leq 1.1$, $-10^\circ \leq \Delta\phi \leq 10^\circ$; in (a2), $0.9 \leq m \leq 1.2$, $-10^\circ \leq \Delta\phi \leq 10^\circ$; in (a3), $0.9 \leq m \leq 1.2$, $-10^\circ \leq \Delta\phi \leq 10^\circ$, based on the input images' tag patterns as described in section II. The directions, spacing, thickness, and shape of the resulting tag lines fit those in the input image quite well. Figure 7c shows the results of a HARP-based method. This method is described in [2]. The myocardium contours are added manually for better readability. Here we find that the tags we reconstruct are more representative of the true tags than the isosurfaces of the phase image recovered from HARP. The Gabor filter bank method is much more robust for large local deformations compared to HARP. Also the result of our method has a better human readability. Without the manually drawn myocardium contours, one can still roughly discern the cardiac region. This is because the HARP's bandpass filter does not have constraints in the spatial domain, and its phase image is very sensitive to artifacts.

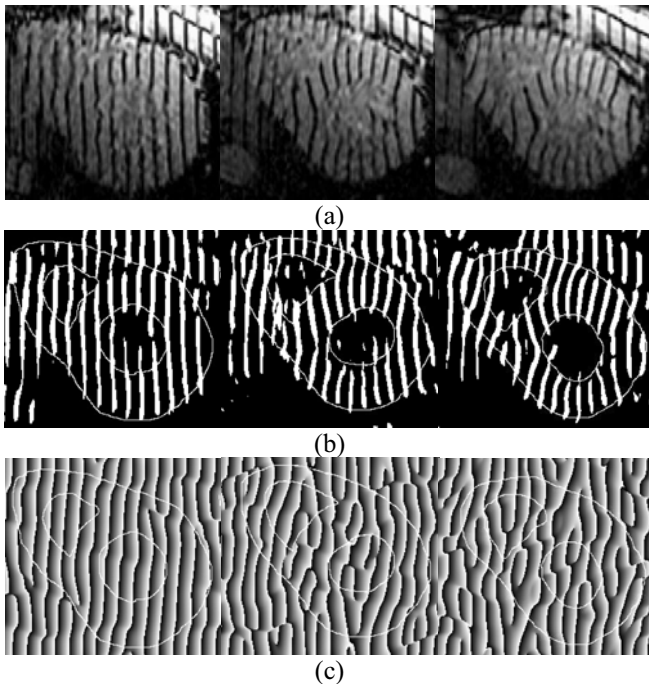


Figure 7: (a) Three tagged cardiac MR images in short axis. They are taken from a MRI sequence during systole. (b) The

output results of our method. (c) HARP-based method result. The myocardium contours are drawn manually for better readabilities.

IV. CONCLUSION And DISCUSSION

In this paper, we have demonstrated how a Gabor filter bank can be used for the segmentation and extraction of cardiac tagging lines. Compared to the HARP method, our method is more reliable and accurate, especially when large tag deformations occur.

In our algorithm, the most essential step is modifying parameters to design the Gabor filter bank. Actually the modification of the Gabor filters' parameters is based on the input image's spatial characteristics. In addition, the modified parameters give us a good way to understand and analyze the cardiac deformations. For instance, the angle modulation $\Delta\theta$ gives the rigid body rotation of the tags and the tissues, and the magnitude modulation m of the tag spacing gives the strain component perpendicular to the tags. This might be a good way to do motion and strain analysis in the future work.

V. REFERENCES

- [1] N. F. Osman, J. L. Prince, "Angle images for measuring heart motion from tagged MRI," *Proc. IEEE Int'l Conf. Image Proc.*, Chicago IL, Oct. 4-7, 1998.
- [2] N. F. Osman, J. L. Prince, "On the design of the bandpass filters in harmonic phase MRI," *Proc. IEEE Int'l Conf. Image Proc.*, Vancouver, Sept. 10-20, 2000.
- [3] D. Dunn, W. E. Higgins, J. Wakeley, "Texture segmentation using 2-D Gabor elementary functions," *IEEE Trans. Pattern Anal. and Machine Intell.*, 16, 130-149, 1994.
- [4] T. P. Weldon, W. E. Higgins, D. F. Dunn, "Efficient Gabor filter design for texture segmentation," *Pattern Recognition*, vol. 29, no. 12, pp. 2005-2016, Dec. 1996.
- [5] T. P. Weldon, W. E. Higgins, "An algorithm for designing multiple Gabor filters for segmenting multi-textured images," *Proc. IEEE Int'l Conf. Image Proc.*, Chicago IL, vol.3. pp. 333-337, Oct. 4-7, 1998.
- [6] R. Mehrotra, K. R. Namuduri, N. Ranganathan, "Gabor filter-based edge detection," *Pattern Recognition*, 25, 1479-1493, 1992.
- [7] J. Daugman, "Uncertainty relation for resolution in space, spatial frequency, and orientation optimized by two-dimensional visual cortical filters," *J. Opt. Soc. Am. A*, vol. 2, no. 7, pp. 1160-1169, July 1985.
- [8] A. Montillo, D. Metaxas, L. Axel, "Automated segmentation of the left and right ventricles in 4D cardiac SPAMM images," *MICCAI* (1) 2002: 620-633.
- [9] Y. Chen, A.A. Amini, "A MAP framework for tag line detection in SPAMM data using markov random fields on the B-spline solid," *Mathematical Methods in Biomedical Image Analysis*, 2001: 131-138.